

等离子体光栅诱导击穿光谱检测土壤重金属元素

施沈城¹, 胡梦云^{1,2,3*}, 张青山¹, 曾和平^{1,2,3}¹华东师范大学精密光谱科学与技术国家重点实验室, 上海 200062;²华东师范大学重庆研究院精密光学重庆市重点实验室, 重庆 401120;³上海理工大学光电信息与计算机工程学院上海市现代光学系统重点实验室, 上海 200093

摘要 搭建了等离子体光栅诱导击穿光谱(plasma-grating-induced breakdown spectroscopy, GIBS)系统对土壤样品进行分析,并与光丝诱导击穿光谱(filament-induced breakdown spectroscopy, FIBS)系统进行对比,成功得到 2 倍左右的谱线信号增强,该谱线信号增强与脉冲间的延时密切相关。此外,通过研究不同激光能量下样品空间位置改变对谱线信号的影响,证明了 GIBS 系统样品最优激发位置范围虽然相比于 FIBS 系统有所减小,但是其不会像 FIBS 系统一样随激光能量的改变而改变。对土壤中重金属元素 Cr 进行了定量研究,发现 FIBS 与 GIBS 系统都能够建立线性的定标曲线,其中 FIBS 系统的检出限为 55.09×10^{-6} ,而 GIBS 系统的检出限为 29.96×10^{-6} ,表明 GIBS 技术具有更高的探测灵敏度。

关键词 光谱学; 激光诱导击穿光谱技术; 光丝; 等离子体光栅; 检出限; 重金属

中图分类号 O433.4

文献标志码 A

DOI: 10.3788/CJL202249.1311002

1 引言

激光诱导击穿光谱(laser-induced breakdown spectroscopy, LIBS)技术是一种新型的光谱分析技术,其将高能脉冲激光聚焦到样品表面进行激发产生等离子体,然后使用光谱仪收集分析等离子体所发射的光谱,从而实现对物质成分的定性或定量分析。相比于高效液相色谱法、电感耦合等离子体质谱法、X 射线荧光法以及原子吸收和发射光谱法等传统分析方法,LIBS 技术具有简单、快速、可现场原位检测以及同时进行多种元素的在线分析等诸多优点,并已经在环境检测^[1-2]、工业生产^[3-4]、生物医学^[5-6]和文物鉴定^[7]等众多领域中得到应用。但是,基于纳秒脉冲对样品进行激发的传统纳秒激光诱导击穿光谱(nanosecond-laser-induced breakdown spectroscopy, ns-LIBS)技术,在光谱分析时会受到基体效应的影响,总体分析结果的稳定性、精度以及灵敏度都有待提高。目前已经有许多改进方法被提出来解决这些问题,如气体辅助法^[8]、等离子体约束法^[9]、纳米颗粒增强法^[10]、光丝诱导击穿光谱技术(filament-induced breakdown spectroscopy, FIBS)^[11]以及等离子体光栅诱导击穿光谱技术(plasma-grating-induced breakdown spectroscopy, GIBS)^[12]。其中,FIBS 技术与 GIBS 技术是基于飞秒激光的改进方法,相比于其他方法,无需

引入额外装置或样品处理步骤。

FIBS 技术中的激发源是飞秒光丝,它是飞秒激光在介质中传播时克尔自聚焦效应与等离子体散焦效应平衡的结果,表现为一条长而稳定的等离子体通道。当在空气中传播时,通道内部的激光功率密度会由于功率钳制效应而被限制为 $5 \times 10^{13} \text{ W/cm}^2$,因此 FIBS 分析时具有较高的稳定性并可以实现远程遥感探测,但功率钳制效应也会限制其谱线信号强度的提升。两束飞秒光丝非共线相互作用之后形成的等离子体光栅正好能够突破这一限制^[12-16],使得等离子体通道中的功率密度以及电子密度提升一个数量级以上。由此发展出来的 GIBS 技术已经被证明能够实现等离子体寿命的延长并有效提高谱线信号强度^[12],同时该研究也指出,基于飞秒激光激发的 FIBS 技术与 GIBS 技术可以有效改善探测时的基体效应。但是等离子体光栅相比于光丝,其等离子体通道的长度显著减短,所以 GIBS 的分析稳定性以及其对探测灵敏度的影响仍待研究。本文选用常见的土壤样品作为分析对象,研究了 GIBS 系统中光谱强度随着脉冲间的延时以及样品空间位置的变化,并与 FIBS 系统进行比较,证明了脉冲间的延时对等离子体光栅的形成非常重要,最终会影响到谱线信号增强的效果。此外,虽然形成的等离子体光栅的长度相比于光丝有所减小,对应的激发谱线的范围有所减小,但是其最优样品激发位置更为稳

收稿日期: 2021-10-18; 修回日期: 2021-11-18; 录用日期: 2021-11-25

基金项目: 国家自然科学基金重点项目(62035005)、国家自然科学基金仪器项目(11727812)

通信作者: *myhu@phy.ecnu.edu.cn

定。最后,我们还通过建立定标曲线,利用定量分析方法证明了相对于 FIBS 系统,GIBS 系统有助于提高探测灵敏度。

2 实验系统装置

GIBS 系统装置示意图如图 1(a)所示,采用美国 Coherent 公司的飞秒激光器作为光源,其中心波长为 800 nm,脉冲宽度为 45 fs,重复频率为 1 kHz。激光器产生的飞秒脉冲经过电控快门、衰减片之后由反射镜反射到分束片(BS)上进行分束,得到能量相等的两束飞秒脉冲。这两束飞秒脉冲经过多次反射之后分别被石英透镜 L_1 (焦距 $f=200$ mm)以及 L_2 (焦距 $f=200$ mm)会聚成丝,并在焦点处相交。基于由伺服电机平移台和反射镜组成的延时线(delay line),控制其中一路飞秒脉冲所走过的光程,使得两束激光同时到达焦点处发生相互作用,形成的飞秒等离子体光栅对样品进行激发。样品被置于由伺服电机平移台组成的三维位移平台上,可通过软件控制与电控快门配合,为

每次脉冲激发提供新的样品表面,并且可以控制样品相对于透镜焦点的位置。石英透镜 L_3 ($f=50$ mm)和 L_4 ($f=50$ mm)组成的收集系统被安装在一个三维调整架上,整个收集系统被调整到最优位置以确保将等离子体的光谱信号耦合至光纤中,并传输至光谱仪完成光谱的分光与探测。其中光谱仪的测量波长范围为 200~975 nm,分辨率为 0.1 nm,其探测器是分辨率为 1024 pixel×1024 pixel 的增强型电荷耦合器件(ICCD)。

光谱仪采集时序原理示意图如图 1(b)所示,由于等离子体与飞秒脉冲不会发生相互作用,前期不会有较强的连续谱线,因此无需设置光谱采集延时,光电探测器(PD)接收到飞秒脉冲后产生的触发信号传输到 ICCD 时便开始光谱采集。而飞秒激光所产生的等离子体寿命为 200~400 ns,采集门宽(t_g)设置为 200 ns^[12]。并且由于飞秒激光较高的重复频率,在采集时可以设置片上积分模式,设置曝光时间为 0.1 s,一次曝光对应 100 条谱线的累加。

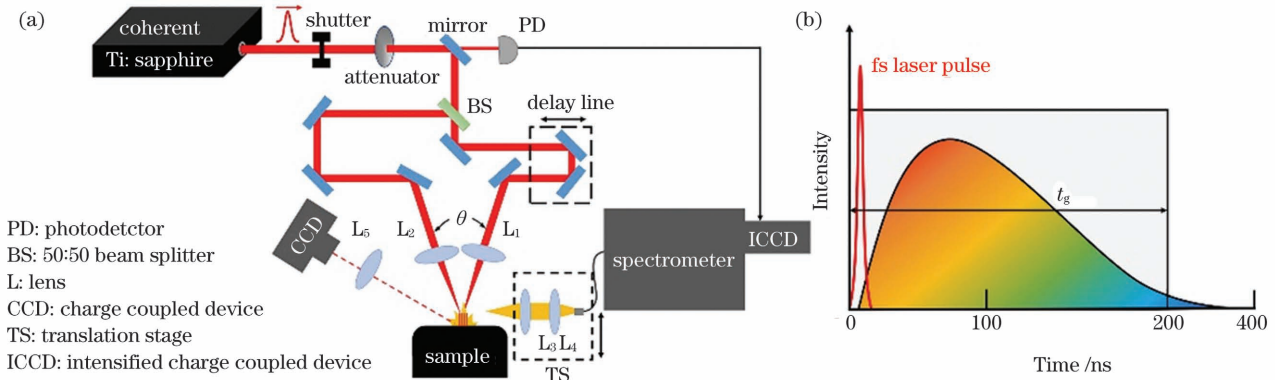


图 1 等离子体光栅诱导击穿光谱系统。(a)装置示意图;(b)光谱采集时序示意图

Fig. 1 Plasma-grating-induced breakdown spectroscopy system. (a) Schematic of experimental setup; (b) schematic of spectrum acquisition timing

此外,GIBS 装置还包括一个由石英透镜 L_5 ($f=100$ mm)和电荷耦合器件(CCD)组成的成像系统,用来观察样品表面相对于透镜焦点的位置,其原理示意图如图 2 所示。在我们的系统中,低能量的飞秒激光可以作为天然的指示激光。样品位置 1 正好处于两束飞秒激光重合区域附近,此时在 CCD 上只能观察到 A 点,如图 2(b)所示;而样品位置 2 则偏离重合区域,此时能够在 CCD 上观察到 B 点和 C 点,如图 2(c)所示。因此只需控制样品表面的前后位置,使得 CCD 上两个像点重合即可确保样品正好处于两束光的重合区域,无需设置参考点位置,简化了寻找样品最优激发位置的过程。

所搭建的 GIBS 系统中两束光丝的夹角在 9.8° 左右,等离子体光栅周期的计算公式^[17]为

$$\Lambda = \lambda / 2 \sin(\theta / 2), \quad (1)$$

式中: Λ 为等离子体光栅周期; λ 为激光波长; θ 为光丝间的夹角。根据式(1),可以计算出等离子体光栅的周期在 $4.6 \mu\text{m}$ 左右。由于两束光丝夹角较小,其中

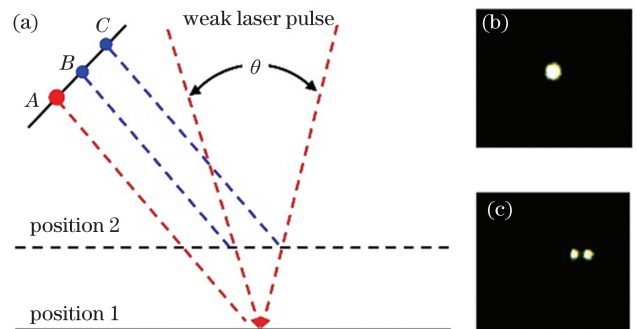


图 2 样品表面监测。(a)监测原理示意图;(b)样品处于两束光重合区域中时的 CCD 像;(c)样品处于两束光重合区域外时的 CCD 像

Fig. 2 Sample surface monitoring. (a) Schematic of monitoring principle; (b) CCD image of sample in overlapping area of two beams; (c) CCD image of sample outside overlapping area of two beams

单束光丝可近似视为与样品垂直,因此通过挡住 GIBS 系统中的一路光,可将系统转化为 FIBS 系统。

3 样品准备

实验使用在中国标准物质网上购买的标准土壤(编号为 GSS-09 和 GBW03121)作为样品。所有样品首先在球磨机中球磨 3 h 进行细化和均匀化处理。其中,在土壤标样 GBW03121 中加入 Cr_2O_3 (质量分数为 99%) 粉末进行均匀掺杂,Cr 元素的质量分数分别为 341×10^{-6} , 729×10^{-6} , 1212×10^{-6} , 1789×10^{-6} , 2147×10^{-6} , 2543×10^{-6} 。每种样品取 0.3 g 倒入到直径为 13 mm 的模具中进行压片处理。液压机在 6 MPa 下进行 1 min 压片,得到表面均匀的土壤样品压片。

4 实验结果分析

4.1 信号增强及脉冲间的延时的影响

我们首先对比了 FIBS 和 GIBS 的谱线信号强度。实验都选取未掺杂的 GSS-09 作为样品,激光能量均设置为 1.5 mJ。取信噪比以及稳定性良好的 Si I 288.2 nm 特征峰进行比较,结果如图 3 所示。从图 3 中可以看到,在相同激光能量下,基于 GIBS 系统获得的谱线信号强度是 FIBS 系统中的 2 倍左右,这与文献[12]中描述的一致,这说明我们所搭建的 GIBS 系统对样品的激发是等离子体光栅对样品的激发,而不是两束光丝激发的简单相加。

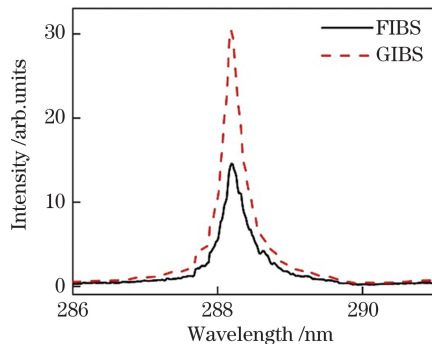


图 3 FIBS 与 GIBS 系统的谱线信号对比

Fig. 3 Spectral comparison between FIBS and GIBS systems

为了进一步证明该观点,我们通过控制延时线来给两束脉冲之间加入延时,延时改变步长设置为 20 fs,与使用的飞秒脉冲宽度接近。同时定义了增强

因子 $I_{\text{GIBS}}/I_{\text{FIBS}}$ (I_{GIBS} 为 GIBS 系统激发样品获得的谱线信号强度, I_{FIBS} 为 FIBS 系统激发样品获得的谱线信号强度),其与脉冲间的延时的关系如图 4 所示。当脉冲延时在 0 fs 附近时,增强因子最大,此时获得的光谱信号为两束光相互作用形成的等离子体光栅对样品的激发。而随着脉冲间的延时的增加,增强因子逐渐下降并趋于 1,说明加入较大脉冲间的延时之后,两束光的相互作用减弱,等离子体光栅消失,此时获得的光谱信号变为两次光丝激发的简单相加。

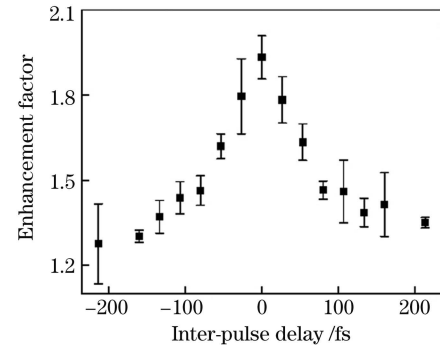


图 4 增强因子随脉冲间延时的变化

Fig. 4 Relationship between enhancement factor and inter-pulse delay

4.2 样品位置对谱线信号的影响

在一般的 ns-LIBS 实验中,不平整样品表面会影响谱线信号的稳定性^[18-19],而样品相对于透镜焦点位置的改变对谱线信号的影响能够有效反映出 LIBS 系统对表面不平整样品的分析稳定性。在 ns-LIBS 技术中,一般需要将焦点控制在样品表面下方 2 mm 左右的位置以获取最优谱线信号^[20]。由于光丝具有长且稳定的等离子体通道,因此在 FIBS 系统中,样品相对于透镜焦点位置的改变对谱线的影响显著减小^[21-24]。而关于 GIBS 系统尚未有这方面的报道。本节将研究对比 FIBS 与 GIBS 系统中样品相对于透镜焦点位置的改变对谱线信号的影响。选取未掺杂的 GSS-09 土壤样品,在激光能量为 0.5, 1.0, 1.5 mJ 三种情况下进行实验,实验时光谱收集系统可以进行调节以获得最优的谱线信号。取 Si I 288.2 nm 特征峰进行比较,实验结果如图 5 所示,其中图 5(a)代表 FIBS 系统而

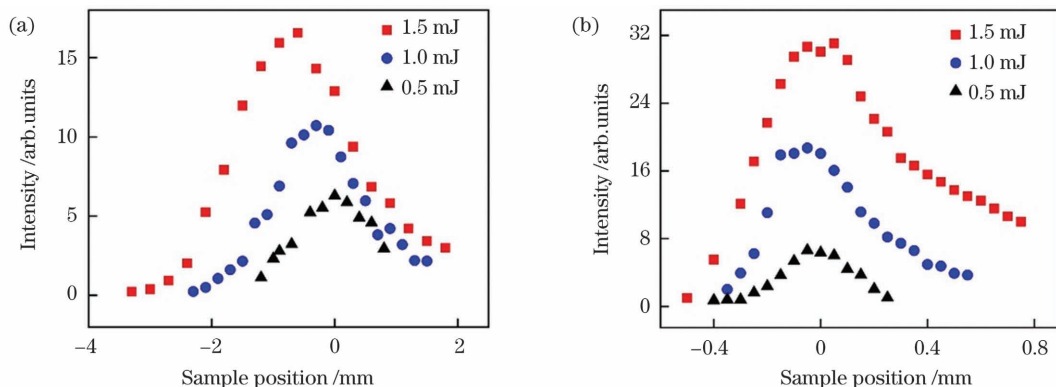


图 5 不同系统中 Si I 288.2 nm 谱线强度随着土壤样品空间位置的变化。(a)FIBS 系统;(b)GIBS 系统

Fig. 5 Si I 288.2 nm spectral line intensity versus sample position in different systems. (a) FIBS system; (b) GIBS system

图 5(b)代表 GIBS 系统,横坐标代表样品与透镜焦点的相对位置,负号代表靠近透镜的方向。可以看到,当激光能量都为 0.5 mJ 时,FIBS 系统中样品在 $-0.5 \sim 0.5$ mm(约为 1 mm 范围)内都有明显的谱线信号激发现象,且这个谱线信号强度的变化趋势与文献[25]中描述的类似,而在 GIBS 系统中,这个区间变为 $-0.1 \sim 0.1$ mm(约为 0.2 mm 范围)。这是由于 GIBS 系统中作为激发源的等离子体光栅是两束光丝相互作用的结果,其长度相比于单光丝有明显减小,但重合区域由于光丝的宽度而具有一定的长度,形成的等离子体光栅具有一定的空间大小,意味着 GIBS 系统激发的谱线也具有较好的稳定性。并且随着激光能量从 0.5 mJ 增加到 1.5 mJ,可以发现,FIBS 系统中样品被激发的范围从原来的 1 mm 左右增加到 4 mm 左右,而 GIBS 系统中样品被激发的范围从原来的 0.2 mm 增加到 0.4 mm,这说明了光丝和等离子体光栅的长度会随着飞秒激光的能量增加而增加。

除此之外,从图 5(a)中可以看到,FIBS 系统中的最优谱线所对应的样品位置随着激光能量的增加从原来的 0 mm 移动到了 -0.5 mm 左右,即朝着透镜方向移动了 0.5 mm,这是由于光丝会在透镜焦点附近形成,但是其具体开始形成的位置会随着激光能量的增加而提前^[26]。从图 5(b)中可以观察到,GIBS 系统中的最优谱线所对应的样品空间位置始终在 0 mm 附近,几乎不随激光能量改变。这是因为等离子体光栅只在两个光丝相互作用的区域中形成,而这只与光路有关,受激光能量的影响较小。GIBS 系统配合所搭建起来的成像系统能够快速确保样品处于光丝相交区

域,这意味着在实际应用中该系统可以快速找到激发最优谱线信号对应的样品位置。

4.3 定量分析

建立定标曲线是 LIBS 常用的定量分析方法,而定标曲线的参数能反映一个 LIBS 系统的定量分析能力。本节将通过对比 FIBS 和 GIBS 系统的定量分析能力。选取配制的不同 Cr 元素浓度的 GBW03121 土壤样品进行实验,实验时控制激光能量为 1.5 mJ,在同一实验条件下重复 5 次后取平均并进行误差计算。根据特征峰 Cr I 425.4 nm 的强度来进行建立定标曲线。实验结果如图 6 所示,其中图 6(a)代表 FIBS 系统,图 6(b)代表 GIBS 系统。可以看到,两个系统都成功建立起了线性的定标曲线。此外,表 1 给出了相应的拟合方程以及参数,其中 I 为特征峰 Cr I 425.4 nm 的谱线强度, x 为样品中 Cr 元素的浓度, R^2 为拟合曲线的线性相关系数, L_{OD} 为计算得到的检出限。可以看出,FIBS 和 GIBS 系统的定标曲线的 R^2 都超过了 0.99,具有良好的线性度。常用的检出限计算公式^[27]为

$$L_{OD} = 3\sigma/s, \quad (2)$$

式中: σ 为同一实验条件下多次采集的 425.1 nm 处的空白信号的标准偏差; s 为定标曲线的斜率。利用式(2)计算检出限,得出 FIBS 的检出限为 55.09×10^{-6} ,而 GIBS 的检出限为 29.96×10^{-6} 。说明在相同的实验条件下,通过搭建 GIBS 系统,可以提高检测的灵敏度,这是由于飞秒等离子体光栅突破了单光丝的功率钳制效应,能对样品进行更有效的激发,这与 4.1 节中的谱线信号增强相对应。

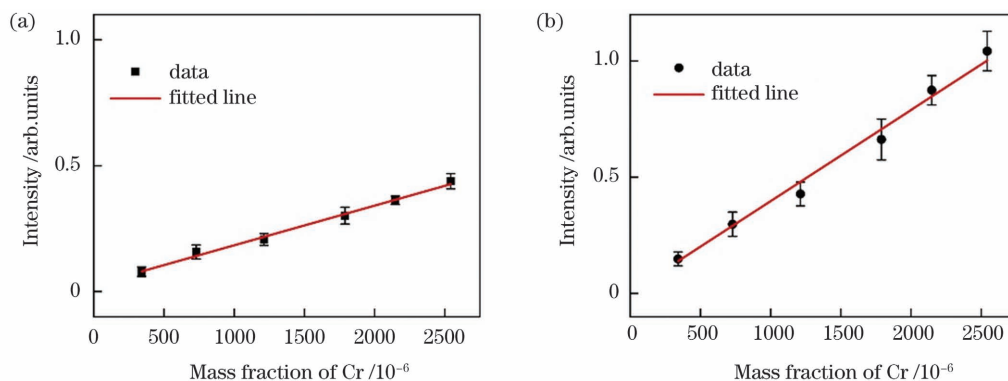


图 6 不同系统中 Cr 元素定标曲线的建立。(a)FIBS 系统;(b)GIBS 系统

Fig. 6 Establishment of Cr element calibration curve in different systems. (a) FIBS system; (b) GIBS system

表 1 定标曲线参数的对比

Table 1 Comparison of calibration curve parameters

System	Calibration curve	R^2	$L_{OD}/10^{-6}$
FIBS	$I = 1.58x + 260$	0.996	55.09
GIBS	$I = 3.92x + 53$	0.990	29.96

5 结论

在相同实验条件下对土壤样品进行对比分析,发现相比于 FIBS 系统,GIBS 系统的谱线强度成功实现

了接近 2 倍的增强,同时证明了该增强会显著受到脉冲间的延时的影响。通过研究谱线强度随样品空间位置的变化,发现等离子体光栅的空间尺寸相比于单束光丝有明显的缩短,但是其仍然具有一定的空间长度,所以 GIBS 系统也具有较好的分析稳定性。除此之外,还发现最优激发位置在 FIBS 系统中会随着激光能量的增加而向透镜方向偏移,而在 GIBS 系统中则始终稳定在两束光丝相互作用区域,不会随着激光能量的改变而改变。这意味着通过配合所搭建的成像系

统,能够更加容易找到样品最优激发位置。最后比较了两个系统对土壤中 Cr 元素建立的定标曲线,计算得出 FIBS 系统的检出限为 55.09×10^{-6} ,而 GIBS 系统的检出限为 29.96×10^{-6} ,说明 GIBS 技术可以提高探测灵敏度。

参 考 文 献

- [1] 石焕, 赵南京, 王春龙, 等. 应用激光诱导击穿光谱测量水体中痕量重金属锌[J]. 激光与光电子学进展, 2012, 49(1): 013003.
Shi H, Zhao N J, Wang C L, et al. Measurement of trace heavy metal zinc in water by laser induced breakdown spectroscopy[J]. Laser & Optoelectronics Progress, 2012, 49(1): 013003.
- [2] 孟德硕, 赵南京, 刘文清, 等. 土壤钾元素的激光诱导击穿光谱定量检测分析[J]. 中国激光, 2014, 41(5): 0515003.
Meng D S, Zhao N J, Liu W Q, et al. Quantitative measurement and analysis of potassium in soil using laser-induced breakdown spectroscopy[J]. Chinese Journal of Lasers, 2014, 41(5): 0515003.
- [3] 沈跃良, 姚顺春, 潘刚, 等. 粘合剂对激光诱导击穿光谱技术测量粉煤灰未燃碳的影响[J]. 中国激光, 2014, 41(3): 0315003.
Shen Y L, Yao S C, Pan G, et al. Influence of binder on laser-induced breakdown spectroscopy measurement of unburned carbon in fly ash[J]. Chinese Journal of Lasers, 2014, 41(3): 0315003.
- [4] 尚栋, 孙兰香, 齐立峰, 等. 基于循环变量筛选非线性偏最小二乘的 LIBS 铁矿浆定量分析[J]. 中国激光, 2021, 48(21): 2111001.
Shang D, Sun L X, Qi L F, et al. Quantitative analysis of laser-induced breakdown spectroscopy iron ore slurry based on cyclic variable filtering and nonlinear partial least squares[J]. Chinese Journal of Lasers, 2021, 48(21): 2111001.
- [5] Rehse S J, Mohaidat Q I, Palchoudhuri S. Towards the clinical application of laser-induced breakdown spectroscopy for rapid pathogen diagnosis: the effect of mixed cultures and sample dilution on bacterial identification[J]. Applied Optics, 2010, 49(13): C27-C35.
- [6] 章琳颖, 黎静, 饶洪辉, 等. 基于 LIBS 的黄龙病脐橙元素检测与品质鉴别[J]. 激光与光电子学进展, 2020, 57(23): 233002.
Zhang L Y, Li J, Rao H H, et al. LIBS-based element detection and quality identification of huanglongbing navel oranges[J]. Laser & Optoelectronics Progress, 2020, 57(23): 233002.
- [7] Ramil A, López A J, Yáñez A. Application of artificial neural networks for the rapid classification of archaeological ceramics by means of laser induced breakdown spectroscopy (LIBS)[J]. Applied Physics A, 2008, 92(1): 197-202.
- [8] Bai X S, Ma Q L, Motto-Ros V, et al. Convolved effect of laser fluence and pulse duration on the property of a nanosecond laser-induced plasma into an argon ambient gas at the atmospheric pressure[J]. Journal of Applied Physics, 2013, 113(1): 013304.
- [9] 杨彦伟. 磁场约束提高 LIBS 定量分析精度研究[J]. 激光与红外, 2019, 49(8): 945-949.
Yang Y W. Study on the quantitative analysis of magnetic field-enhanced LIBS[J]. Laser & Infrared, 2019, 49(8): 945-949.
- [10] de Giacomo A, Gaudiuso R, Koral C, et al. Nanoparticle-enhanced laser-induced breakdown spectroscopy of metallic samples[J]. Analytical Chemistry, 2013, 85(21): 10180-10187.
- [11] Harilal S S, Yeak J, Phillips M C. Plasma temperature clamping in filamentation laser induced breakdown spectroscopy[J]. Optics Express, 2015, 23(21): 27113-27122.
- [12] Hu M Y, Peng J S, Niu S, et al. Plasma-grating-induced breakdown spectroscopy[J]. Advanced Photonics, 2020, 2: 065001.
- [13] Yang X, Wu J, Tong Y Q, et al. Femtosecond laser pulse energy transfer induced by plasma grating due to filament interaction in air[J]. Applied Physics Letters, 2010, 97(7): 071108.
- [14] Yang X, Wu J, Peng Y, et al. Plasma waveguide array induced by filament interaction[J]. Optics Letters, 2009, 34(24): 3806-3808.
- [15] Lu P F, Wu J, Zeng H P. Manipulation of plasma grating by impulsive molecular alignment[J]. Applied Physics Letters, 2013, 103(22): 221113.
- [16] Liu F J, Yuan S, He B Q, et al. Enhanced stimulated Raman scattering by femtosecond ultraviolet plasma grating in water[J]. Applied Physics Letters, 2018, 112(9): 094101.
- [17] Bernstein A C, McCormick M, Dyer G M, et al. Two-beam coupling between filament-forming beams in air[J]. Physical Review Letters, 2009, 102(12): 123902.
- [18] 徐进力, 胡梦颖, 张鹏鹏, 等. 高压制样-LIBS 技术测定土壤样品中稀土元素的应用研究[J]. 光谱学与光谱分析, 2020, 40(12): 3806-3811.
Xu J L, Hu M Y, Zhang P P, et al. Application of high pressure pelletised sample and LIBS in the determination of rare earth elements in soil samples[J]. Spectroscopy and Spectral Analysis, 2020, 40(12): 3806-3811.
- [19] 雷鹏达, 付洪波, 易定容, 等. 激光诱导击穿光谱表征熔覆层缺陷程度[J]. 中国激光, 2020, 47(4): 0411001.
Lei P D, Fu H B, Yi D R, et al. Characterization of cladding defects via laser-induced breakdown spectroscopy[J]. Chinese Journal of Lasers, 2020, 47(4): 0411001.
- [20] 潘立剑, 陈蔚芳, 周晏锋, 等. 基于响应面法的激光诱导击穿光谱实验装置参数优化研究[J]. 中国激光, 2020, 47(9): 0911001.
Pan L J, Chen W F, Zhou Y F, et al. Parameter optimization of laser-induced breakdown spectroscopy experimental device based on response surface methodology[J]. Chinese Journal of Lasers, 2020, 47(9): 0911001.
- [21] Ackermann R, Stelmaszczyk K, Rohwetter P, et al. Triggering and guiding of megavolt discharges by laser-induced filaments under rain conditions[J]. Applied Physics Letters, 2004, 85(23): 5781-5783.
- [22] Chin S L, Xu H L, Luo Q, et al. Filamentation "remote" sensing of chemical and biological agents/pollutants using only one femtosecond laser source[J]. Applied Physics B, 2009, 95(1): 1-12.
- [23] Liu W, Xu H L, Méjean G, et al. Efficient non-gated remote filament-induced breakdown spectroscopy of metallic sample[J]. Spectrochimica Acta Part B: Atomic Spectroscopy, 2007, 62(1): 76-81.
- [24] Rohwetter P, Stelmaszczyk K, Wöste L, et al. Filament-induced remote surface ablation for long range laser-induced breakdown spectroscopy operation[J]. Spectrochimica Acta Part B: Atomic Spectroscopy, 2005, 60(7/8): 1025-1033.
- [25] 高勋, 杜闯, 李丞, 等. 基于飞秒激光等离子体丝诱导击穿光谱探测土壤重金属 Cr 元素含量[J]. 物理学报, 2014, 63(9): 095203.
Gao X, Du C, Li C, et al. Detection of heavy metal Cr in soil by the femtosecond filament induced breakdown spectroscopy[J]. Acta Physica Sinica, 2014, 63(9): 095203.
- [26] Brodeur A, Chien C Y, Ilkov F A, et al. Moving focus in the propagation of ultrashort laser pulses in air[J]. Optics Letters, 1997, 22(5): 304-306.
- [27] Niu S, Zheng L J, Khan A Q, et al. Laser-induced breakdown spectroscopic detection of trace level heavy metal in solutions on a laser-pretreated metallic target[J]. Talanta, 2018, 179: 312-317.

Plasma Grating Induced Breakdown Spectroscopic Detection of Heavy Metal Elements in Soil

Shi Shencheng¹, Hu Mengyun^{1,2,3*}, Zhang Qingshan¹, Zeng Heping^{1,2,3}

¹ State Key Laboratory of Precision Spectroscopy, East China Normal University, Shanghai 200062, China;

² Chongqing Key Laboratory of Precision Optics, Chongqing Institute, East China Normal University, Chongqing 401120, China;

³ Shanghai Key Laboratory of Modern Optical System, School of Optical-Electrical and Computer Engineering, University of Shanghai for Science and Technology, Shanghai 200093, China

Abstract

Objective Laser-induced breakdown spectroscopy (LIBS) is a novel atomic-emission spectroscopic technique, which has many advantages such as multi-elemental detection, rapid response for online monitoring, and easy sample preparation for in situ measurements, and it has been applied in many fields. However, nanosecond laser-induced breakdown spectroscopy (ns-LIBS) still has some defects such as poor stability, low analysis accuracy, and matrix effects. Many methods have been proposed to solve these problems. Among them, filament-induced breakdown spectroscopy (FIBS) and plasma-grating-induced breakdown spectroscopy (GIBS) based on femtosecond laser excitation do not require the introduction of additional equipment and sample preparation steps if compared with other methods. In FIBS, a long and stable filament is used to ablate samples. And it has been proved that FIBS has very stable analysis results and can be used to realize remote sensing detection. And GIBS is based on the plasma grating formed by the interaction of two non-collinear filaments to excite samples. A significant increase in spectral line intensity has been successfully observed in the comparative experiment between FIBS and GIBS. However, the length of the plasma grating is greatly reduced compared with that of the filament, so it is necessary to investigate the analysis stability of the GIBS technology. In addition, the influence of the enhanced spectral line intensity brought by the GIBS technology on the detection limit is still to be studied.

Methods We build a GIBS system based on a plasma grating formed by the interaction of two filaments intersecting at a small angle to ablate the sample and generate plasma. In order to better control the experimental variables, we realize the conversion to the FIBS system by blocking one of the light filaments in the GIBS system. The sample is placed on a three-dimensional translation table to avoid over-ablation and the position of the sample relative to the focal point of the lens is changed. We collect the light emission from the induced plasma and transmit it to a spectrometer by an optical fiber. The light dispersed by the spectrometer is detected with an intensified charge-coupled device (ICCD). The ICCD is set to an on-chip integration mode to realize 100 excitations for each spectral data. In addition, we also configure the standard soil samples with different concentrations of Cr to establish calibration curves and analyze the detection limits of these two systems.

Results and Discussions We first compare the signal intensities of the spectral lines induced by the FIBS system and the GIBS system under the same conditions. An enhancement factor of around 2 is successfully obtained, which is very sensitive to the inter-pulse delay (Fig. 4). From this perspective, it can be clearly judged that the GIBS system we build is based on the excitation of the sample by the plasma grating formed by the interaction of two filaments. Then we study the influence of sample spatial position on these two systems to reflect the stability of the excited sample. When the laser energy is increased from 0.5 mJ to 1.5 mJ, the sample spatial position range corresponding to the obvious spectral line signal excited in the FIBS system increases from 1 mm to 4 mm, while in the case of GIBS system, such a range increases from 0.2 mm to 0.4 mm (Fig. 5). Unsurprisingly, the GIBS system has stricter requirements on the sample spatial location than the FIBS system. However, as laser energy increases, the optimal spectral line signal position in the GIBS system is stable around 0 mm, the position where the filaments intersect. In contrast, the optimal spectral line signal position in the FIBS system moves towards the lens as laser energy increases. In the last part, we compare the detection sensitivities of the FIBS system and the GIBS system by establishing a calibration curve for Cr element in the soil. In both systems, the coefficient of determination (R^2) of the calibration curve exceeds 0.99 (Table 1), which means that both systems are very suitable for a quantitative analysis. But what is more, the limit of detection (LOD) in the FIBS system is calculated to be 55.09×10^{-6} , while in the GIBS system it is 29.96×10^{-6} . This shows that the GIBS system is more advantageous for the detection of trace elements.

Conclusions We build a GIBS system to analyze soil samples, and the spectral signal enhancement by about 2 times that of the FIBS system is successfully obtained, which is closely related to the inter-pulse delay. By studying the influence of the spatial position of the sample on the spectral line signal under different laser energies, it is proved that although the

sample spatial position range corresponding to the obvious spectral line signal excited in the GIBS system is reduced compared with that in the FIBS system, the optimal spectral line signal position in the GIBS system does not change with laser energy, as that in the FIBS system. In addition, in the quantitative study of the heavy metal element Cr in the soil, it is found that both FIBS and GIBS systems can be used to establish a linear calibration curve and the limit of detection in the FIBS system is 55.09×10^{-6} , while the limit of detection in the GIBS system is 29.96×10^{-6} , indicating that the GIBS technology has high detection sensitivity.

Key words spectroscopy; laser-induced breakdown spectroscopy; filament; plasma grating; limit of detection; heavy metal